Bohmian Mechanical Trajectories for the Simple Harmonic Oscillator

Matthew Lawyer

A senior thesis submitted to the faculty of
Brigham Young University
in partial fulfillment of the requirements for the degree of

Bachelor of Science

Jean-François Van Huele, Advisor

Department of Physics and Astronomy

Brigham Young University

October 2020

ABSTRACT

Bohmian Mechanical Trajectories for the Simple Harmonic Oscillator

Matthew Lawyer
Department of Physics and Astronomy, BYU
Bachelor of Science

We give an outline of the importance and historical development of Bohmian mechanics, an ontological interpretation of quantum theory, followed by an exposition of its mathematical formulation. We then use Bohmian mechanics to obtain plots of trajectories and of the time evolution of the Bohmian mechanical quantum potential for the simple harmonic oscillator. We show how an already formed classical intuition can be relied on to help understand the behavior of the trajectories through their dynamical relationship to the quantum potential.

Keywords: quantum mechanics, quantum interpretation, Bohmian mechanics, de Broglie-Bohm theory, ontological interpretation, simple harmonic oscillator, quantum potential, trajectories

ACKNOWLEDGMENTS

Many thanks to Jean-François Van Huele for the freedom granted in selecting and developing this project, and for the encouragement and support in wrestling with complex ideas. Thanks also to Kenneth Leitham, who first showed me what I am capable of. Thanks especially to my wife Laura, who has been more patient than I deserve as I have worked on this research.

Contents

Chapter 1

Ontology in Quantum Mechanics

1.1 Ontology and Epistemology

The mathematics of quantum mechanics was developed empirically as a tool for explaining and predicting experimental results. The resultant machinery is probabilistic in nature. The tools it provides predict the outcomes of experiments with high accuracy, but give us few clues as to the correspondence between elements of the mathematical formulation and reality. Because the theory was developed empirically as a tool for predicting experimental results, it is unable to give a description of certain processes in nature, e.g. the transition from one quantum state to another, or the "collapse" of the wave function—processes which are out of our current experimental reach. As a result, it can be argued that quantum theory is incomplete.

The origin of this view is often attributed to Albert Einstein, since he argued for such a position [1]. Niels Bohr is credited with arguing for a different view, now known as the *Copenhagen* interpretation of quantum mechanics: that quantum mechanics tells us all that can be known about a quantum system, and that attempts to find a more complete description cannot be fruitful. Historically, these two views have been considered to be in opposition. However, careful thought

reveals that this need not be the case. The first view is a statement regarding that which *exists*, while the second concerns that which *can be known*. While these must be consistent wherever they overlap, clearly all that exists need not be known.

The word *ontology* describes the study of that which is. The word *epistemology* describes the study of knowledge and our acquisition of it. The above views can be stated in these terms. Einstein's view was that quantum mechanics is incomplete ontologically, while Bohr believed it is complete epistemologically. This is discussed in greater detail, and in very enlightening fashion, by E. T. Jaynes [2], and all are recommended to read the sections of his talk concerning the EPR paradox. In addition, the second chapter of Bohm and Hiley's *The Undivided Universe* [3] provides much insight regarding the issue. For the purposes of this discussion, it is sufficient to quote only a few sentences from Jaynes in summary:

> Bohr and Einstein could never understand each other because they were thinking on different levels. When Einstein says [quantum mechanics] is incomplete, he means it in the ontological sense; when Bohr says [quantum mechanics] is complete, he means it in the epistemological sense. Recognizing this, their statements are no longer contradictory.

As is further discussed by Jaynes, most physicists misunderstood Bohr's position, and the common notion has come to be that what quantum mechanics tells us is all that *exists*. The apparent opposition of these two views stems from the misunderstanding outlined here. However, there really is no contradiction between them.

The only real question regarding the topic is whether one view of quantum theory is better aligned with the aims of theoretical physics. It is the opinion of the author that science is best served when the theoretician concerns himself with ontology—with attempting to understand what is *really there*—and not with simply describing his perceived limits of knowledge. This is principally because to focus on the limits of our knowledge restricts *a priori* the avenues of thought which

may be explored. To exclude the pursuit of an ontological description of reality on grounds of its being considered fruitless is to close the door to any possible future discovery along that avenue of thought, and so the door must only be closed if well justified. Certainly this justification could not be based on the kind of misconception outlined above.

Though there are many solutions which have been proposed to the problem of describing reality ontologically, we will focus here on only one, called Bohmian mechanics and developed by David Bohm in 1952 [4]. Bohmian mechanics describes reality as a quantum field coupled with particles, so that particle-wave duality is not seen as one entity behaving both as a particle and a wave, but rather as two entities—a particle and a wave—combining to give rise to the phenomena we observe. It describes particles existing continuously with well-defined position and momentum governed by a *quantum potential*, so that the statistical nature of quantum experiments is only due to our ignorance of initial particle position. Thus, the Bohmian mechanical quantum picture consists of ensembles of trajectories, of which a single trajectory is selected based on initial particle position.

The use of Bohmian mechanics to conceptualize quantum phenomena has several advantages. First, the tools that it provides can open the door to discoveries which otherwise would be missed. This is true because the trajectories encode information about the system which is otherwise neglected. This is demonstrated in several works [5, 6, 7, 8]. Additionally, as is alluded to in the previous paragraph, Bohmian mechanics opens the door to theory which is out of the reach of canonical quantum mechanics. One article from *The Royal Society* analyzes the emergence of the Born rule from the dynamics of Bohmian mechanics, and predicts a time scale for this emergence [9]. Another article from *Nature* proposes an experiment involving the statistical distribution of arrival times for spin-$\frac{1}{2}$ particles [10]. Neither of these are accessible to the canonical quantum mechanics due to the interpretation's lack of a time operator. Lastly, the grounding of quantum theory in ontology (i.e. grounding it in the language of what physically exists) gives us an easily accessible set of tools—the dynamical relationship between the quantum potential and the trajectories—through

which to visualize the dynamics of quantum processes and intuitively understand them by relying on our already well-formed classical intuition. This last point is primarily of pedagogical value, but is also of use to researchers and others who simply want to be well informed. Bohmian mechanics gives a coherent picture of quantum dynamical processes so that the measurement paradox and Schrödinger's cat paradox are resolved before they ever arise, and the mysteries of the double slit experiment and of EPR are made plain. The picture given by Bohm's interpretation disallows the public confusion and mysticism surrounding quantum phenomena in the public eye.

This thesis is dedicated to the analysis of the simple harmonic oscillator (SHO) from the Bohmian mechanical perspective. The SHO is solved in every introductory course on quantum mechanics, and is an excellent approximation to many systems occurring in nature. For these reasons, it is an excellent starting point for the ontological study of quantum theory from both a practical and a pedagogical point of view. Though the SHO is not addressed by Bohm, it is discussed by Peter Holland [11] and Gary Bowman [12], which the reader can reference for additional perspectives. Section 1.2 provides historical context for the development of Bohmian mechanics, along with a brief discussion on the importance of Bell's inequality in regard to Bohmian mechanics. Section 2.1 gives a brief exposition of the tools used by Bohmian mechanics, after which numerically generated plots of Bohmian trajectories in the SHO are presented and analyzed in depth in Section 2.2. Section 3 gives a brief conclusion to the discussion. A summarized version of this work will be published in the *Journal of the Utah Academy of Science, Arts, and Letters* [13].

The reader interested in better understanding any of the topics discussed above, including the benefits of giving priority to ontology in physics, can reference the aforementioned sections of the works by Jaynes [2] and Bohm [3]. For an easy introduction to Bohmian mechanics and Bohmian mechanical thinking, see Roderich Tumulka's paper [14] (structured as a dialogue). For general exposition of Bohmian mechanics, the reader can reference Bohm's works [3, 4], as well as Peter Holland's excellent book [11]. A good resource treating the use of Bohmian mechanics as a

modeling tool is Wyatt's *Quantum Dynamics with Trajectories* [15].

1.2 Historical Background

In 1951, David Bohm published one of the classic texts on quantum theory [16]. Unsatisfied with certain aspects of the standard interpretation, he developed his own interpretation [4], which he published in 1952. His ideas are now known as *Bohmian mechanics*.

Though he was unaware of the fact at the time he developed them, his ideas were similar to previous ideas held by Louis de Broglie and Nathan Rosen. de Broglie published in 1927 what he called the *theory of the double solution* [17]. This double solution consisted of a wave solution to the Schrödinger equation, as well as singular solutions corresponding to localized point particles. He presented his double solution the same year at the Solvay congress in a simplified form which he called *pilot wave theory* [18]. He was unable to respond to objections raised, especially by Wolfgang Pauli, and, convinced that his approach could not lead to a viable interpretation of quantum mechanics, he abandoned his work. Because of this, Bohmian mechanics is sometimes called de Broglie-Bohm theory, the de Broglie-Bohm interpretation, or pilot wave theory.

Rosen published in 1945 [19], drawing less attention than de Broglie. His ideas are very similar to those of Bohm in their mathematical form. Like de Broglie, he believed his ideas to be unviable and abandoned them.

Bohm's dissatisfaction with aspects of quantum theory was held by others, most prominently Albert Einstein, Boris Podolsky, and Nathan Rosen, together referred to as EPR. As mentioned in Section 1.1, in 1935 they published a paper, now known as the EPR paper, which is still famous today [1]. In that paper they argue that any theory describing the objectively real world must be able to simultaneously describe all real properties of the objects with which it is concerned. In essence, they assert that any theory must be both real and local. Here, *realism* means that entities in the

world exist continuously, even when not being observed, and *locality* means that all influences are communicated locally from point to point (i.e. no superluminal influences). Because this is not a feature of quantum mechanics, they concluded that quantum theory must be incomplete. In this context, completion of the theory would entail the introduction of *hidden variables* to the theory, so called because they are quantities presumed to exist but so far hidden to our observation.

This view contrasted with the thinking of other physicists of the time. In 1932, John von Neumann published a book containing a proof that hidden variables cannot exist[1] [21]. In the following years, several other *no hidden variables* theorems are developed by other physicists, some of which are addressed in [22].

In his work, Davin Bohm refutes comments made by both Pauli and von Neumann (see Appendix B of [4], part II). Having theorems proving the nonviability of hidden variable theories, as well as having what looked like a coherent counterexample to these theorems, quantum theory needed some definitive resolution. In 1964, John Bell responded to the EPR sentiment with a theoretical test for nonlocality in nature, known as Bell's theorem [23]. In this work he gives a constraint, in the form of an inequality, on the correlations between two entangled particles. This constraint was developed with the simultaneous assumptions of locality and realism. Thus, if nature permits the kinds of hidden variables advocated by EPR, all observations made experimentally must satisfy Bell's inequality. Detailed discussion on the dependence of Bell's inequality on these assumptions can be found in Appendix A. Bell's ideas were developed by John Clauser, Michael Horne, Abner Shimony, and Richard Holt (CHSH) into a realisable experiment [24, 25]. In addition to providing us with this theoretical test, John Bell also refuted several no hidden variables theorems, including that of von Neumann [22].

The first experimental test of Bell's theorem, called a Bell test, was performed in 1972 using the CHSH form of the Bell's inequality [26]. This experimental test, together with Bell's 1964 work,

[1] For a much more accessible exposition of von Neumann's proof, see [20].

proved that nature must be either nonlocal or nonreal, excluding the possibility of local hidden variables. Since then, additional, more rigorous Bell tests have been carried out, closing theoretical loopholes in the logic of Bell's argument [26, 27, 28, 29].

It is important to note that Bell's theorem only excludes the simultaneous state of locality and realism, but does not exclude either on its own. Thus, only *local* hidden variable interpretations are excluded, while any interpretation employing *nonlocal* hidden variables (representing realism without locality) are allowed. Bohm's interpretation is a nonlocal hidden variable interpretation (in which continuous particle position is the unobserved *hidden* quantity), and so is consistent with Bell's work[2]. This point is often misunderstood. Many authors present interpretations like Bohm's as naive and as having been already disproven experimentally. Bell's work is often used as justification for this claim. As is discussed here, and in more detail in Appendix A, this is incorrect. Any interpretation which aims to keep locality can do so if it forfeits realism. Likewise, realism can be preserved by forfeiture of locality.

[2]It is humorous that position is regarded as a "hidden" variable, since position is actually the quantity observed in all quantum measurements. Other "observables," such as energy, momentum, and spin, are never measured, but are inferred from specialized position measurements. It would seem more appropriate, then, to regard position as the only *real* variable, while regarding the rest to be hidden.

Chapter 2

Bohmian Mechanical Trajectories

In Section 2.1 the mathematical tools used by Bohm will be described. Then, in Section 2.2, numerical plots generated using these tools will be analyzed.

2.1 Mathematical Formulation of Bohmian Mechanics

The purpose of this section is to impart an understanding of Bohmian mechanics sufficient to understand the topics discussed throughout the remainder of the document. Only single-particle systems in one dimension will be treated. Readers interested in further details regarding the Bohmian mechanical machinery can refer to Bohm's 1952 papers [4] and his 1993 book [3], upon which works this exposition is based.

Let $\Psi : \mathbb{R}^4 \longrightarrow \mathbb{C}$ represent an arbitrary single-particle wave function in space $\mathbf{x} \in \mathbb{R}^3$ and time $t \in \mathbb{R}$. The behavior of the wave function Ψ for a particle of mass m in the presence of an external potential $V(\mathbf{x},t)$ is governed by the Schrödinger equation,

$$i\hbar\frac{\partial\Psi}{\partial t} = -\frac{\hbar^2}{2m}\nabla^2\Psi + V(\mathbf{x},t)\Psi, \tag{2.1}$$

where $\hbar$ is Planck's constant. In polar form, factorizing the amplitude $R(\mathbf{x},t)$ and the phase $S(\mathbf{x},t)$,

Ψ can be written as

$$\Psi(\mathbf{x},t) = R(\mathbf{x},t)e^{i\frac{S(\mathbf{x},t)}{\hbar}}, \tag{2.2}$$

where $R : \mathbb{R}^4 \longrightarrow \mathbb{R}$ and $S : \mathbb{R}^4 \longrightarrow \mathbb{R}$ are real-valued functions of position and time. Plugging (2.2) into (2.1) and separating the real and imaginary parts, we obtain

$$\frac{\partial R^2}{\partial t} + \nabla \cdot \left(R^2 \frac{\nabla S}{m} \right) = 0, \tag{2.3}$$

and

$$\frac{\partial S}{\partial t} + \frac{\left(\nabla S\right)^2}{2m} + V(\mathbf{x},t) - \frac{\hbar^2}{2m}\frac{\nabla^2 R}{R} = 0. \tag{2.4}$$

Equation (2.3) is a conservation equation of probability, with $|\Psi|^2 = R^2$ the probability density. Equation (2.4) is of more immediate interest to us, having a form similar to the classical Hamilton-Jacobi equation:

$$\frac{\partial S_{cl}}{\partial t} + \frac{\left(\nabla S_{cl}\right)^2}{2m} + V(\mathbf{x},t) = 0, \tag{2.5}$$

where S_{cl} is the classical negative time integral of energy.

Indeed, (2.4) differs from (2.5) in form only in the addition of the term

$$Q(\mathbf{x},t) = -\frac{\hbar^2}{2m}\frac{\nabla^2 R}{R}, \tag{2.6}$$

which must have units of energy. Bohm refers to (2.6) as the *quantum potential*, while referring to V as the *classical potential*. Defining the *total potential* as $U(\mathbf{x},t) = V(\mathbf{x},t) + Q(\mathbf{x},t)$ and substituting this expression into (2.4), we see that its form exactly matches that of (2.5).

Hamilton-Jacobi theory, from which (2.5) is derived, is a formulation of classical mechanics equivalent to Newtonian mechanics [30]. Thus, by associating (2.4) and (2.5), we justify the use of tools provided by Hamilton-Jacobi theory, taking into account the additional information contained in (2.6), to obtain quantities of interest. In particular, we identify S with S_{cl} in order to obtain particle velocity $\mathbf{v}$ from momentum

$$\mathbf{p}(\mathbf{x},t) = m\mathbf{v}(\mathbf{x},t) = \nabla S(\mathbf{x},t)$$

$$\implies \mathbf{v}(\mathbf{x},t) = \frac{\nabla S(\mathbf{x},t)}{m}, \tag{2.7}$$

where S is determined by (2.4). In the one-dimensional case, the vector $\mathbf{v}$ becomes the scalar v, the vector $\mathbf{x}$ becomes the scalar x, and the gradient operator ∇ becomes the partial derivative $\frac{\partial}{\partial x}$ with respect to x.

The vector $\mathbf{v}$, having spatial dependence, describes a time-dependent velocity field. It does not describe any single trajectory, but all possible trajectories simultaneously. The trajectory taken by a given particle is determined by its initial position.

In practice, solving (2.3, 2.4) as a system of equations is difficult. However, as this system is mathematically equivalent to the Schrödinger equation, we can solve (2.1) for Ψ and extract R and S from the polar form (2.2).

For the basis states of a system, finding the polar form is generally straightforward. For a superposition of basis states, we require some additional manipulation to find S. Let $\Psi = \sum_{n=1}^{N} c_n \Psi_n = Re^{iS/\hbar}$, where $\Psi_n = R_n e^{iS_n/\hbar}$. Then

$$\Psi = \sum_{n=1}^{N} c_n R_n e^{iS_n/\hbar} = \sum_{n=1}^{N} c_n R_n \big(\cos(S_n/\hbar) + i\sin(S_n/\hbar)\big)$$

$$= \sum_{n=1}^{N} c_n R_n \cos(S_n/\hbar) + i\sum_{n=1}^{N} c_n R_n \sin(S_n/\hbar) = R\cos(S/\hbar) + iR\sin(S/\hbar). \tag{2.8}$$

Separating the real and imaginary parts of (2.8), we obtain

$$R\cos(S/\hbar) = \sum_{n=1}^{N} c_n R_n \cos(S_n/\hbar) \tag{2.9}$$

and

$$R\sin(S/\hbar) = \sum_{n=1}^{N} c_n R_n \sin(S_n/\hbar). \tag{2.10}$$

Dividing (2.9) by $\cos(S/\hbar)$ and (2.10) by $\sin(S/\hbar)$ results in

$$R = \frac{\sum_{n=1}^{N} c_n R_n \cos(S_n/\hbar)}{\cos(S/\hbar)} = \frac{\sum_{n=1}^{N} c_n R_n \sin(S_n/\hbar)}{\sin(S/\hbar)} \implies \tan(S/\hbar) = \frac{\sum_{n=1}^{N} c_n R_n \sin(S_n/\hbar)}{\sum_{n=1}^{N} c_n R_n \cos(S_n/\hbar)}.$$

Thus, for a superposition of basis states,

$$S = \hbar \arctan\left(\frac{\sum_{n=1}^{N} c_n R_n \sin(S_n/\hbar)}{\sum_{n=1}^{N} c_n R_n \cos(S_n/\hbar)}\right). \tag{2.11}$$

Throughout this discussion we will rely additionally on an extention to the Bohmian situation of the classical law governing acceleration a in terms of potential,

$$a = -\frac{1}{m}\frac{d}{dx}U(x,t), \tag{2.12}$$

to analyze the relationship between the total potential $U(x,t)$ and the trajectories produced by (2.7).

2.2 Bohmian-mechanical SHO

We now apply this method to a single particle in the time-independent potential of the SHO in one dimension. Here, $V(x) = \frac{1}{2}m\omega^2 x^2$, where ω is the classical frequency of oscillation. The time-independent part of the nth basis state of the quantum SHO is given by

$$\psi_n(x) = \frac{1}{\sqrt{n!}}\mathbb{A}^n \psi_0(x), \tag{2.13}$$

where

$$\psi_0(x) = \left(\frac{m\omega}{\pi\hbar}\right)^{\frac{1}{4}} e^{-\frac{m\omega}{2\hbar}x^2}. \tag{2.14}$$

The zeroth state (2.14) is referred to as the *ground state*. Here, the operator $\mathbb{A}$ allows us to find the excited states from the ground state [31]. The time-dependent wave function $\Psi_n(x,t)$ is formed by multiplying $\psi_n(x)$ by a standard time-dependent factor:

$$\Psi_n(x,t) = \psi_n(x)e^{-iE_n t/\hbar}, \tag{2.15}$$

where $E_n = (n+\frac{1}{2})\hbar\omega$ is the energy associated with the nth state [31].

Noting that (2.15) is already in polar form, we can extract S_n directly. Evidently, $S_n(t) = -E_n t$. This is consistent with S_n as the action (the negative time integral of energy), as E_n is constant in time. $S_n(t)$ is constant in space. Thus, for every basis state, including the ground state, we obtain $v(x,t) = \frac{1}{m}\frac{\partial}{\partial x}S_n(t) = 0$. The corresponding trajectories, showing the evolution of one-dimensional position in time, are obtained by numerical application of (2.7) and (2.11), and are plotted in Figure 2.1.

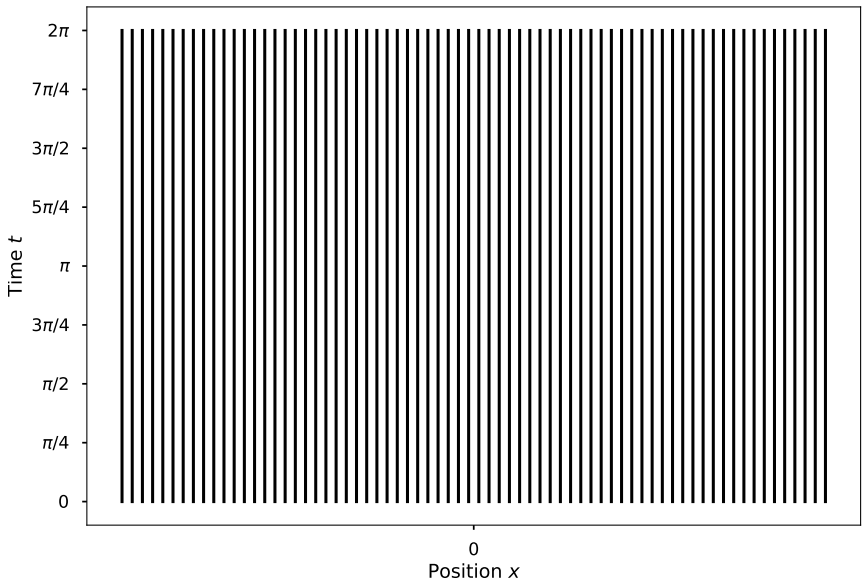

Figure 2.1 Bohmian trajectories for basis states of the SHO ($\Psi(x,t) = \Psi_n(x,t)$). Position is plotted horizontally, and time vertically. Each line represents a distinct trajectory based on a different initial position. As is shown, the SHO basis states exhibit no particle motion.

The trajectories corresponding to basis states exhibit no particle motion—a particle in any basis state is stationary[1]. This contradicts our classical intuition. We expect a particle in a harmonic potential to be stationary only if its initial position is the center of the potential and the initial velocity is zero; otherwise, we expect any displacement from the center or any nonzero initial velocity to produce sinusoidal oscillations with an amplitude determined by the initial displacement or velocity. This serves to highlight the fact that Bohmian mechanics is an interpretation of quantum theory still very different from classical mechanics. The correspondence with the classical oscillator is found in considering the *coherent state* (an oscillatory wave packet consisting of an infinite

[1] It is appropriate that the basis states are often referred to as *stationary states*, though for a different reason.

superposition of eigenstates, considered in detail in [11], as well as on page 24 of this document) and *not* in the behavior of the eigenstates.

The explanation of this behavior is found by considering the quantum potential. A particle which feels a potential will accelerate according to (2.12). In this case, the particle acceleration is dependent not only on the classical potential $V(x) = \frac{1}{2}m\omega^2x^2$, which we specify when we write down the Schrödinger equation, but also on the quantum potential (2.6) which is determined by (2.3, 2.4) *after* we specify the classical potential. The quantum potential corresponding to any stationary state has the form of a negative parabola: $Q(x) = C - \frac{1}{2}m\omega^2x^2, C \in \mathbb{R}$. This can be seen by considering equation (2.4). The first term is constant, and the second term is zero. Thus, the sum of the last two terms must equal a constant (the negative of the first term). From this we see that the total potential must be $U(x) = V(x) + Q(x) = C$. For the ground state, this is illustrated in Figure 2.2.

One may ask how making an energy measurement on an eigenstate of the SHO can result in observation of a nonzero energy if the particles involved are stationary. In quantum mechanics, the term associated with kinetic energy is the first term on the right-hand side of the Schrödinger equation (2.1), an equation describing the wave function, not the associated Bohmian particle. In equation (2.4), this energy is shared between the second term (describing the kinetic energy of the Bohmian particle) and the fourth term (the quantum potential). In this case, the second term is zero, but the energy is still present in the quantum potential.

Superposing states leads to interesting new behavior. In Figure 2.3 the trajectories corresponding to the state $\Psi(x,t) = \frac{1}{\sqrt{2}}\big(\Psi_0(x,t) + \Psi_1(x,t)\big)$ are shown. This state corresponds to the ground state superposed with the first excited state.

At time $t = 0$ the trajectories slightly left of center are evenly spaced but rapidly move to the left, gradually accumulating in a band arcing gently to the left until time $t = \pi$ (in appropriately scaled units of time), at which time the band arcs back to the right and the trajectories spread back

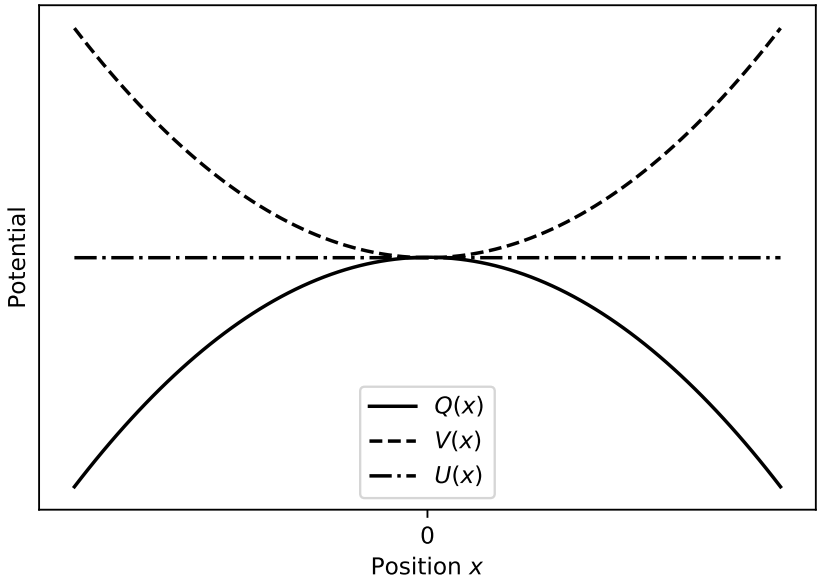

Figure 2.2 For the ground state, the x-dependent term in $Q(x)$ completely cancels the x-dependent term in $V(x)$, resulting in a constant potential.

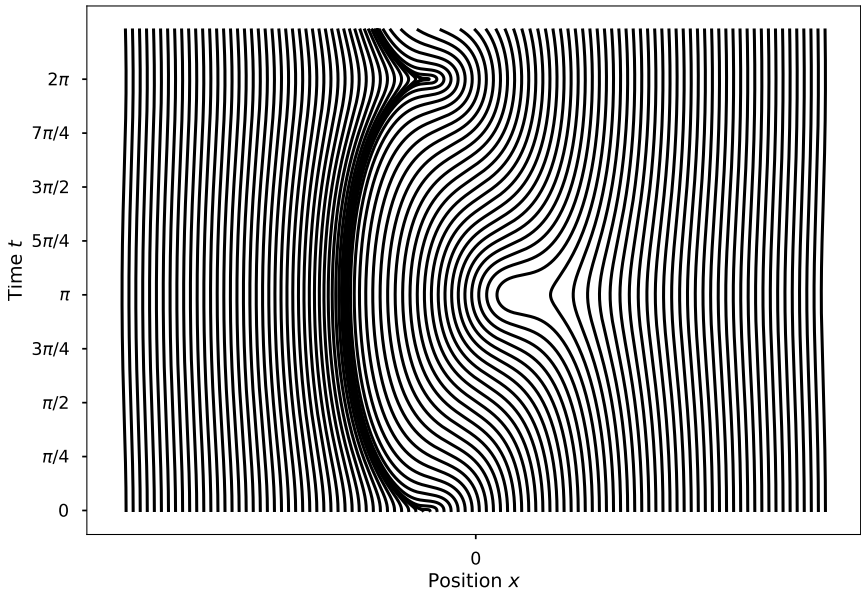

Figure 2.3 Bohmian trajectories for the state $\Psi(x,t) = \frac{1}{\sqrt{2}}\big(\Psi_0(x,t) + \Psi_1(x,t)\big)$. Compare to Figure 2.1.

to their initial positions by time $t = 2\pi$. The trajectories are cyclic with period 2π, so this abrupt spreading and re-accumulation of trajectories at times which are integer multiples of 2π has the visual appearance of a cusp in the plot. In Figure 2.3, slightly more than one cycle is shown in order to make this cusp more visible.

It is interesting to note that none of the trajectories here shown cross. Indeed, this is a general feature of Bohmian mechanics, and not only of this state: trajectories cannot cross. Proof of this

fact can be found in Appendix B. In this case, it is logical to expect that, where trajectories display different velocities, they compress into bands. This feature of Bohmian mechanics will not be discussed further, but the reader is encouraged to keep it in mind as further states are examined.

Just before time $t = \pi$, the trajectories slightly right of center display movement to the left and spread out, then undo this motion just after time $t = \pi$, forming an apparently empty pocket, which when reflected over the time axis has the shape of the cusp formed by the trajectories on the left.

It is important to note that these trajectories are mutually exclusive—if a particle takes one trajectory, it will not take any other. There are infinitely many hypothetical trajectories which can be taken. The one actually taken depends on the initial particle position. We plot only a finite number of hypothetical trajectories to give an approximate map of the velocity field available to the particle. Hence, the density of trajectories at any point depends on the initial sampling. For these trajectories, initial positions were sampled uniformly in x at time $t = 0$. Had initial positions been sampled uniformly in x at time $t = \pi$, we would have a distribution which is evenly spaced at times which are odd-integer multiples of π. The empty pocket on the right would then contain an even sampling of trajectories, which at following times would be compressed into bands, similarly to the way it occurs for trajectories on the left. Similarly, choosing to sample at time $t = \pi/2$ would produce a distribution of trajectories which would favor neither the right nor the left. Thus the band structure on the left is present on the right, though not visible in these plots. This structure is symmetric in space about the center of the potential, though shifted in time across this center point by $\Delta t = \pi$.

Here we remind the reader to keep in mind the fact that Bohmian trajectories cannot cross, in order to better conceptualize the behavior which we analyze. Trajectories near the center of the potential and located between the two band-forming regions are somewhat sinusoidal in form, which we can appreciate in a harmonic potential, and are bounded by the bands, reminiscent of the classical concept of a strict turning point related to energy level. However, these trajectories are not at all what is predicted by the Newtonian theory. Though the collection of trajectories is symmetric

about the center of the potential, individual trajectories are not. Some trajectories even fail to cross the center of the potential altogether. This is especially true of trajectories considerably further from the center of the potential than the bands of accumulation, where trajectories remain nearly stationary. Quantum mechanics tells us that there is a nonzero probability of finding the particle beyond the classical turning points corresponding to its energy. Bohmian mechanics then tells us that, if found there, the particle will never approach the bottom of the classical parabolic potential.

Let us now consider in greater detail the total potential $U(x,t) = V(x,t) + Q(x,t)$ corresponding to this superposition state. The total potential is time dependent. Five constant time plots spaced evenly over one half of one cycle are shown in Figures 2.4a-2.4e. Figure 2.4f adds the quantum and classical potentials for comparrison. In the first frame, there is a singularity slightly left of center. The derivative is positive on both sides of the singularity, so a particle on either side will be accelerated to the left. The slope is steepest near the singularity and drops off quickly on either side, so that the acceleration is greatest near the singularity. Thus the hypothetical trajectories near the singular point will be bent left violently, with the effect dropping off quickly with distance, so that trajectories far off are only slightly drawn to the left. The difference in accelerations here results in a nonzero relative velocity between trajectories, so that the distance between them is reduced and they accumulate in a bundle to the left of the singularity. This singularity exists for a very short span of time, and quickly evolves into a nearly flat potential with a small dip where the singularity once was, so that the rapid accumulation ceases. The derivative is now positive to the right and *negative* to the left of the dip. Trajectories to the right will continue to accelerate gradually to the left until they pass the dip, and trajectories to the left (including those who crossed over from the right) will continue to travel to the left, while accelerating to the right. In the subsequent frames, the dip becomes shallower and migrates to the right side of the center point, where it again deepens. Here, in the last frame, it forms a new singularity, with derivatives opposite those occurring in the singularity on the left in the first frame. Trajectories are now accelerated violently to the right near

the singular point, and more gently further away. The cycle is completed with the repetition of these steps in reverse order, until the conditions again match those of the first frame.

Logically, the behavior of the trajectories which we expect from our analysis of the total potential must match the actual behavior plotted in Figure 2.3. As shown by Bohm, the quantum mechanical phenomena which we observe in the laboratory can be explained in terms of trajectories by statistically averaging the behavior of the trajectories [3]. But our analysis of the behavior of the trajectories from the quantum potential relied only on (2.12). Thus we have shown that, when viewed through the lens of Bohmian mechanics, Newtonian intuition can be used to easily understand the behavior of quantum systems.

Many more interesting states can be analyzed in a similar manner. In the rest of this section we will consider a limited variety of additional quantum states to further illustrate the use of Newtonian intuition for understanding the behavior of Bohmian mechanical systems. First, we consider a state $\Psi(x,t) = \frac{1}{\sqrt{3}}\big(\Psi_0(x,t) + \Psi_1(x,t) + \Psi_2(x,t)\big)$ superposing three basis states instead of two. We will take the ground state superposed with the first two excited states. Trajectories for this state are shown in Figure 2.5. Again we see accumulation of trajectories into a belt with periodic behavior and symmetric structure across the center of the potential.

One important qualitative difference between this state and the state represented in Figure 2.3 is that, where at times which are integer multiples of 2π the trajectories in Figure 2.3 are all swept in the same direction (to the left) as they accumulate into bands, here they are drawn from opposite directions to a central point of accumulation. This feature can again be explained in terms of the quantum potential. The total potential $U(x,t)$ at time $t = 0$ is shown in Figure 2.6a. Similar to what is seen in Figure 2.4a, at time $t = 0$ we have a singularity slightly left of center. However, in this case the derivative has opposite sign on either side of the singular point, so that trajectories everywhere are accelerated to varying degrees towards this point. This effect is more severe for trajectories closer to the singular point. By time $t = \pi/4$, the shape of the potential around the

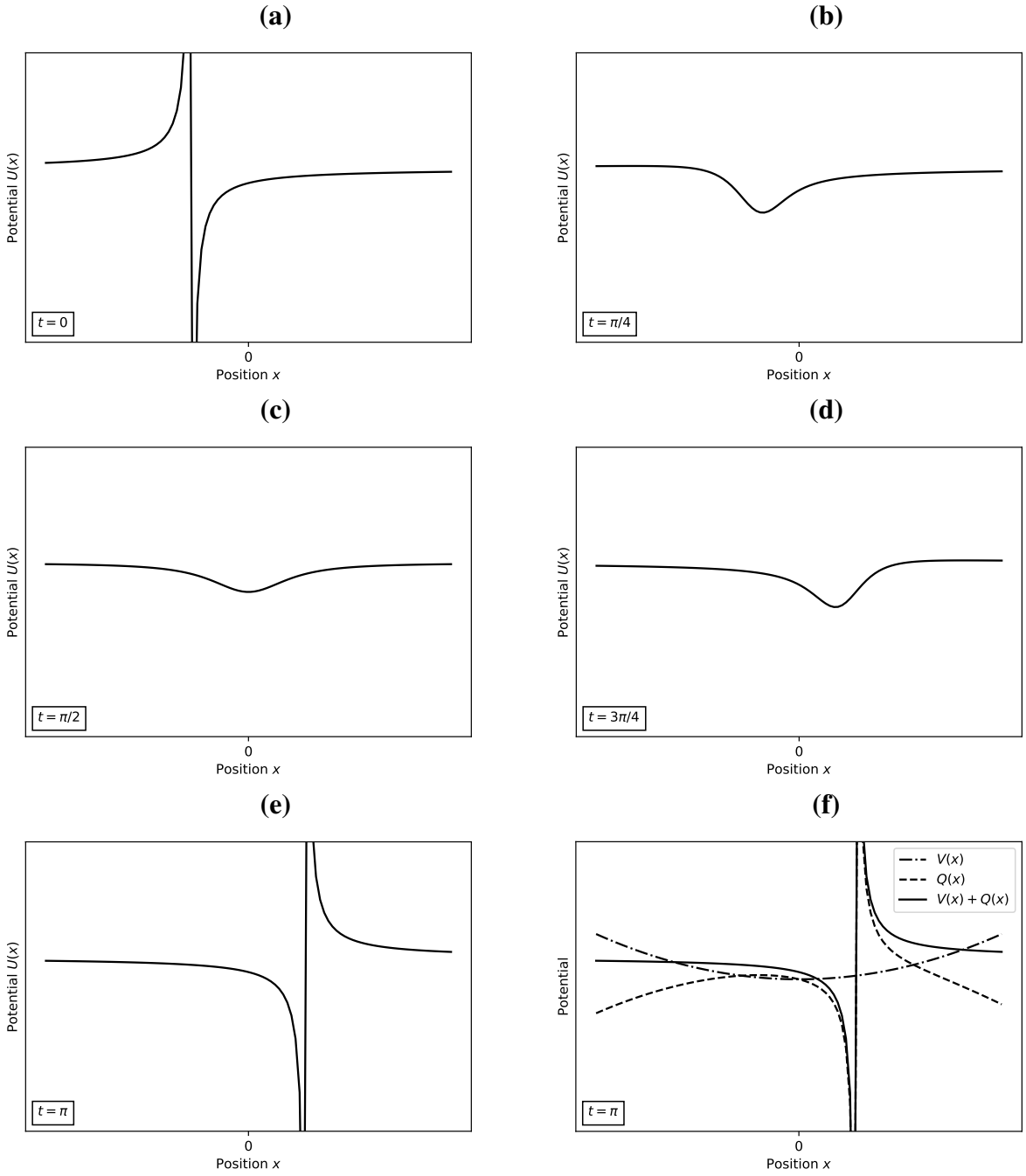

Figure 2.4 In frames 2.4a through 2.4e, the total potential $U(x,t)$ corresponding to the state $\Psi(x,t) = \frac{1}{\sqrt{2}}\big(\Psi_0(x,t) + \Psi_1(x,t)\big)$ is plotted in time increments of $\pi/4$ for $0 \leq t \leq \pi$. In frame 2.4f, the total potential is plotted alongside the quantum and classical potentials at time $t = \pi$ for completeness, showing that $U(x,t) = V(x,t) + Q(x,t)$.

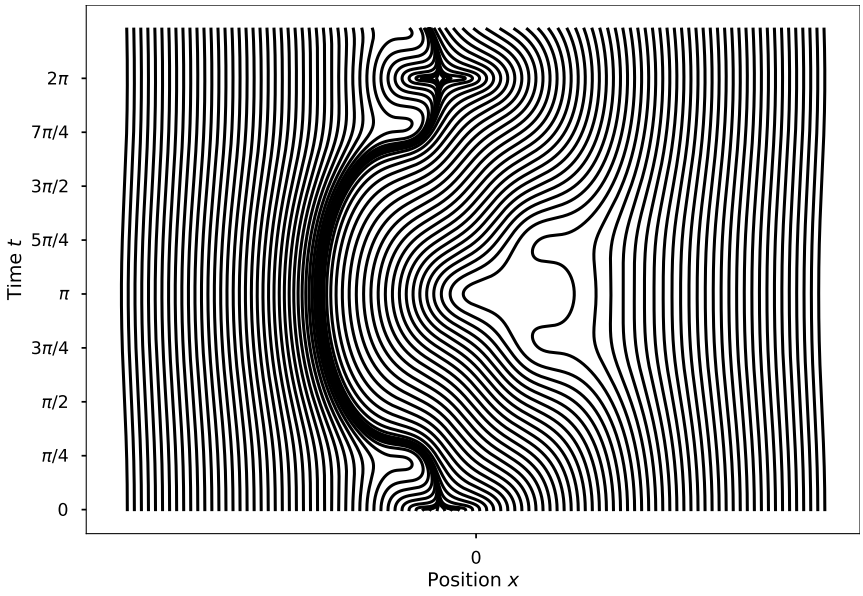

Figure 2.5 Bohmian trajectories for the state $\Psi(x,t) = \frac{1}{\sqrt{3}}\big(\Psi_0(x,t) + \Psi_1(x,t) + \Psi_2(x,t)\big)$. Compare to Figures 2.1 and 2.3.

singularity has changed so as to form two local extrema on either side of the singularity. On the left, this local extremum is also an absolute maximum, so trajectories approaching from the left are reflected back. Note that for this to be the case, the derivative to the left of this maximum point has changed sign. On the right this local extremum is a local maximum, but the potential here is lower than the potential at other points further to the right. Thus, trajectories approaching from the right will be slowed in their approach, but will ultimately overcome this barrier and continue on their path towards the left. Because this local maximum is lower than other values to the right, there must be some local minimum point between the right-hand extremum and the higher-potential zone to its right. This is seen to occur near the center of the potential, and it is observed that the derivative at points immediately to the right of this local minimum is steeper than at the same points at time $t = 0$. Thus, we expect the trajectories approaching from the right to accelerate if they are to the right of this minimum at time $t = \pi/4$, but to decelerate slightly if between this minimum and the adjacent local maximum. Here all trajectories are moving to the left. In frame 2.6c we see that by time $t = \pi/2$ the singularity completely disappears and is reduced to a dip symmetric to the dip left by the local minimum in the previous frame. The derivative to the left of this dip has again changed,

so that the impetus given to the leftmost trajectories is reversed and they are accelerated to the right. Meanwhile, trajectories on the opposite side continue to be accelerated to the left. In frames 2.6d and 2.6e we see both dips migrate to the right, the leftmost one disappearing while the rightmost one deepens to form a singularity. The derivative on the left side of the potential becomes increasingly shallow, so that acceleration to the right of trajectories on the left gradually decreases. In frame 2.6d we see that the deepening right-hand dip is surrounded by local maxima, the right-hand maximum being an absolute maximum, so that trajectories approaching the singularity from the extreme right are reflected, while trajectories to the left of this extreme right region which are able to overcome the potential barrier represented by the left-hand local maximum are temporarily decelerated to the left before being re-accelerated to the left. At time $t = \pi$, we see a singularity to the right of center, symmetric in space to the situation at time $t = 0$, and trajectories on either side are accelerated towards this central point of accumulation. The cycle is again completed by the repetition of frames 2.6a through 2.6e in reverse order, until the situation again resembles that at time $t = 0$. Again, all of this expected behavior is consistent with what is observed in the numerically plotted trajectories in Figure 2.5.

Without changing any weights, simply changing the sign of one of the basis states making up this superposition drastically changes the predicted trajectories. For example, consider the previous case with the coefficient of the second excited state made negative. This is represented in Figure 2.7. Here we see trajectories accumulating into two band-like regions instead of one, each of these having a distinct behavior. Notice that each of these bands is of the unidirectional kind present in Figure 2.3.

The evolution of the total potential $U(x,t)$ corresponding to this state is shown in Figure 2.8. In frame 2.8a, we see two singularities, one slightly to the left of center, and the other a somewhat greater distance to the right of center. Each is of the form present in Figure 2.4a, though the derivative at points immediately surrounding the right-hand singularity has inverted sign. The

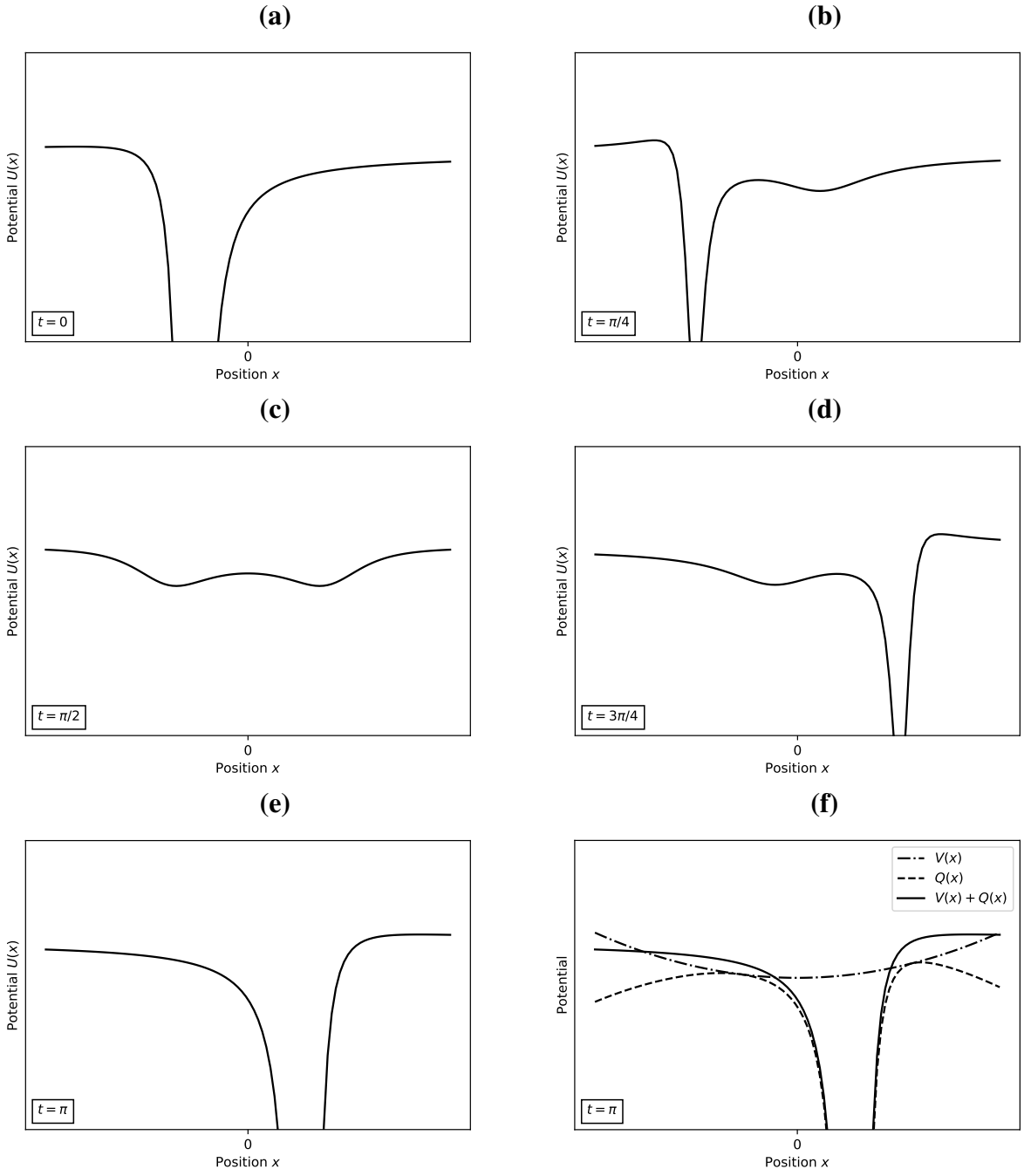

Figure 2.6 In frames 2.6a through 2.6e, the total potential $U(x,t)$ corresponding to the state $\Psi(x,t) = \frac{1}{\sqrt{3}}\big(\Psi_0(x,t) + \Psi_1(x,t) + \Psi_2(x,t)\big)$ is plotted in time increments of $\pi/4$ for $0 \leq t \leq \pi$. In frame 2.6f, the total potential is plotted alongside the quantum and classical potentials at time $t = \pi$ for completeness, showing that $U(x,t) = V(x,t) + Q(x,t)$.

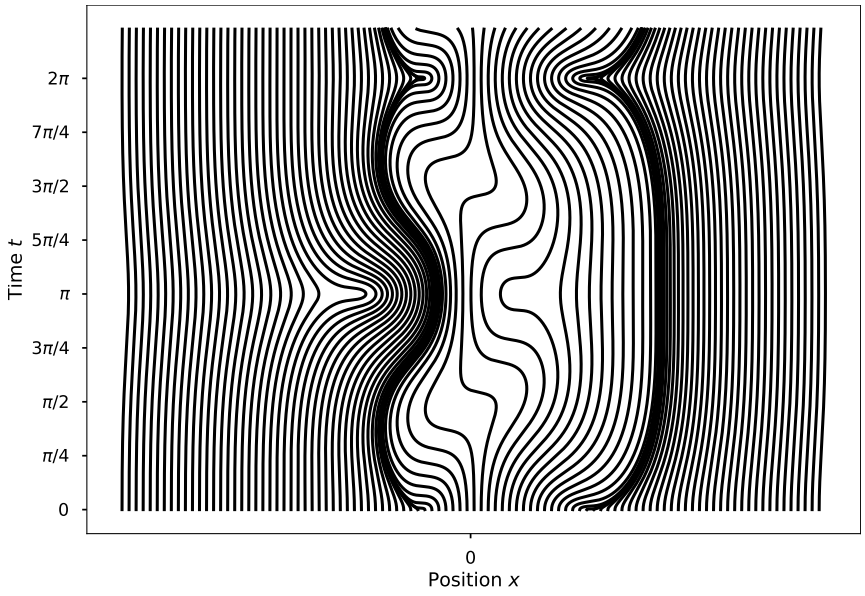

Figure 2.7 Bohmian trajectories for the state $\Psi(x,t) = \frac{1}{\sqrt{3}}\big(\Psi_0(x,t) + \Psi_1(x,t) - \Psi_2(x,t)\big)$. Compare to Figures 2.1, 2.3, and 2.5.

maximum point between these two singularities occurs near the center of the potential ($x = 0$), so we expect all trajectories to the left of center to be accelerated to the left, while all trajectories to the right of center will be accelerated to the right. The effect is greater near the singularities, with the effect dropping off with distance, and as was the case in our analysis of Figure 2.4, this differential results in an accumulation of trajectories due to varying velocities. The magnitude of acceleration is much greater for the left-hand singularity than for the right-hand singularity, as well as shorter-reaching (the effect drops off more quickly with distance). As is again the case in Figure 2.4, these singularities only exist for a brief period of time before disappearing. By time $t = \pi/4$, the right-hand singularity has left behind nothing but a very shallow dip, and the left-hand singularity has left a somewhat more prominent dip. The evolution of the potential at points on the far right-hand side is similar to the evolution of the potential in Figure 2.4, so it is not surprising that the trajectories primarily impacted by the right-hand singularity and its evolution, and specifically the resulting band of accumulated trajectories, have a form similar to the trajectories in Figure 2.3. The left-hand dip in frame 2.8b has the effect of reversing the acceleration of trajectories sent to the left at time $t = 0$. As this dip moves to the right in subsequent frames, trajectories nearer the

center are decelerated and drawn right. By time $t = 3\pi/4$, the right-hand dip has moved to the left of center, and here forms a singularity at time $t = \pi$, so that trajectories on the left are first sent left, then are accelerated right, and are finally accelerated left again as the progression of the total potential prepares to reverse itself to complete the cycle. At the same time, the left-hand dip moves to the right of center and forms a singularity, so that the situation at time $t = \pi$ mirrors that at time $t = 0$. The new singularity on the right is nearer the center than the original singularity on the right at time $t = 0$, and its effect falls off quickly with distance, so that this singularity does not affect the accumulation band formed on the right in the first frames in any significant way. Again, as is expected, the behavior predicted by this analysis coincides with what is seen in Figure 2.7.

To conclude, we will analyze trajectories for two additional, and perhaps more theoretically interesting, states. The first, who's corresponding trajectories are shown in Figure 2.9, is a *coherent state*, which is the quantum state which most closely approximates a classical state. The second, who's trajectories are shown in Figure 2.11, is a *cat state*, so called because it is the superposition of two nearly-classical states (an allusion to the indeterminate condition of Schrödinger's cat).

Note that the principal structures of these ensembles of trajectories possess narrow chaotic regions which accumulate trajectories along their edges, so that at time $t = 2\pi$ holes exist in the distribution of trajectories which did not exist at time $t = 0$. These are artifacts resulting from instabilities in the numerical methods used to generate the figures, and do not represent actual behavior of the system.

The coherent state of the quantum harmonic oscillator is the state whose behavior most closely resembles that of the classical harmonic oscillator. A coherent state is associated with a complex number α such that the energy measured corresponding to the state is $\left(|\alpha|^2 + \frac{1}{2}\right)\hbar\omega$. The coherent state $\Psi^\alpha(x,t)$ corresponding to the constant α can be constructed from basis states according to

$$\Psi^\alpha(x,t) = e^{-\frac{|\alpha|^2}{2}} \sum_{n=0}^{\infty} \frac{\alpha^n}{\sqrt{n!}} \Psi_n(x,t).$$

Since computers are limited to performing finite approximations to infinite sums, we are forced to

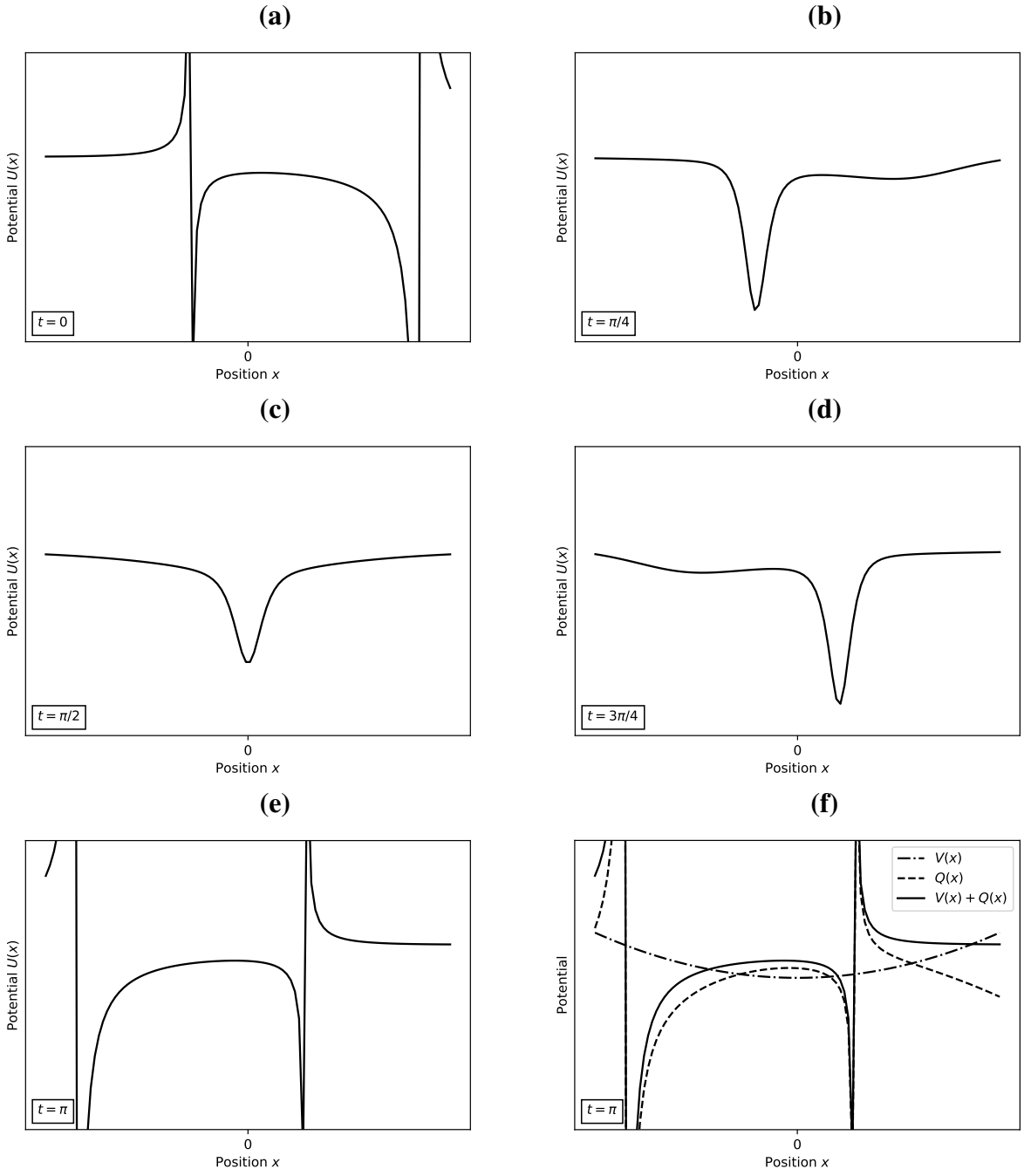

Figure 2.8 In frames 2.8a through 2.8e, the total potential $U(x,t)$ corresponding to the state $\Psi(x,t) = \frac{1}{\sqrt{3}}\big(\Psi_0(x,t) + \Psi_1(x,t) - \Psi_2(x,t)\big)$ is plotted in time increments of $\pi/4$ for $0 \leq t \leq \pi$. In frame 2.8f, the total potential is plotted alongside the quantum and classical potentials at time $t = \pi$ for completeness, showing that $U(x,t) = V(x,t) + Q(x,t)$.

chose some integer N at which to truncate our sum. For $\alpha = 1$, a numerical approximation to the trajectories predicted by Bohm is shown in Figure 2.9. The trajectories in the center of the potential move in what appears to be a sinusoidal fashion—much more so than the trajectories presented in Figure 2.3. These trajectories are smooth and uniform across this central region. Additionally, the region in which trajectories oscillate appears to be bounded much more strictly than for previous states, reminding us of the turning points related to energy in the classical oscillator. All of these features are shared by the classical oscillator, so to see them present here in the trajectories corresponding to the nearest-to-classical quantum state is not surprising. Yet, we still see many trajectories which fail to cross the center of the potential, with nearly stationary trajectories far out on either side (compare with Holland [11]). In fact, all but one of our infinitude of trajectories are asymmetrical about the center.

Figure 2.9 Bohmian trajectories for an approximation to the coherent state $\Psi^1(x,t)$. Note the numerical instabilities.

Because of the necessity of approximation, the potential we calculate will also imperfectly represent the true quantum potential corresponding to the coherent state. For reasons which we have not precisely identified, our approximation of the potential, shown in Figure 2.10, does not correspond as perfectly as we would hope to the approximate trajectories in Figure 2.9. However,

it is still possible to identify general features of the potential corresponding to what is seen in the behavior of the trajectories.

In frame 2.10a the potential is approximately flat on the extreme left and right sides. Between these two regions, the potential has a positive derivative, implying particle acceleration to the left, though it is not uniform throughout this region. The singularity on the right interrupting this central region is probably a result of insufficient approximation of infinity, as is the inequality of the value of the derivative on either side of this singular point. This is similarly true of the non-uniformity of this central region in all frames shown in Figure 2.10. As time progresses, we see the derivative decrease and eventually invert, so that by time $t = \pi$ the situation mirrors that found at time $t = 0$, as seen in frame 2.10e. If we imagine this seesaw behavior in a uniform potential, we expect the acceleration of particles to occur precisely as in Figure 2.9.

A cat state is the superposition of two diametrically opposed states—the simultaneous existence of two incompatible situations—named in reference to the unnatural condition of Schrödinger's cat. The cat state is either even or odd, depending on whether the sum or the difference of the superposed states is taken. For the harmonic oscillator, we can construct a cat state by evenly superposing coherent states for α and $-\alpha$: [2]

$$\Psi^{\alpha}_{even}(x,t) = \frac{1}{\sqrt{2}}\big(\Psi^{\alpha}(x,t) + \Psi^{-\alpha}(x,t)\big),$$

$$\Psi^{\alpha}_{odd}(x,t) = \frac{1}{\sqrt{2}}\big(\Psi^{\alpha}(x,t) - \Psi^{-\alpha}(x,t)\big).$$

The trajectories for the even cat state $\Psi^{1}_{even}(x,t)$ corresponding to $\alpha = 1$ are shown in Figure 2.11. As this state is built from the coherent state, we are again required to plot trajectories of a finite approximation to a true cat state, and we again see numerical instabilities in some regions. It is interesting to note that these trajectories have a period of length π—one half the length of the periods

[2] The trajectories corresponding to $\alpha = -1$ are precisely those shown in Figure 2.9 reflected over the x-axis.

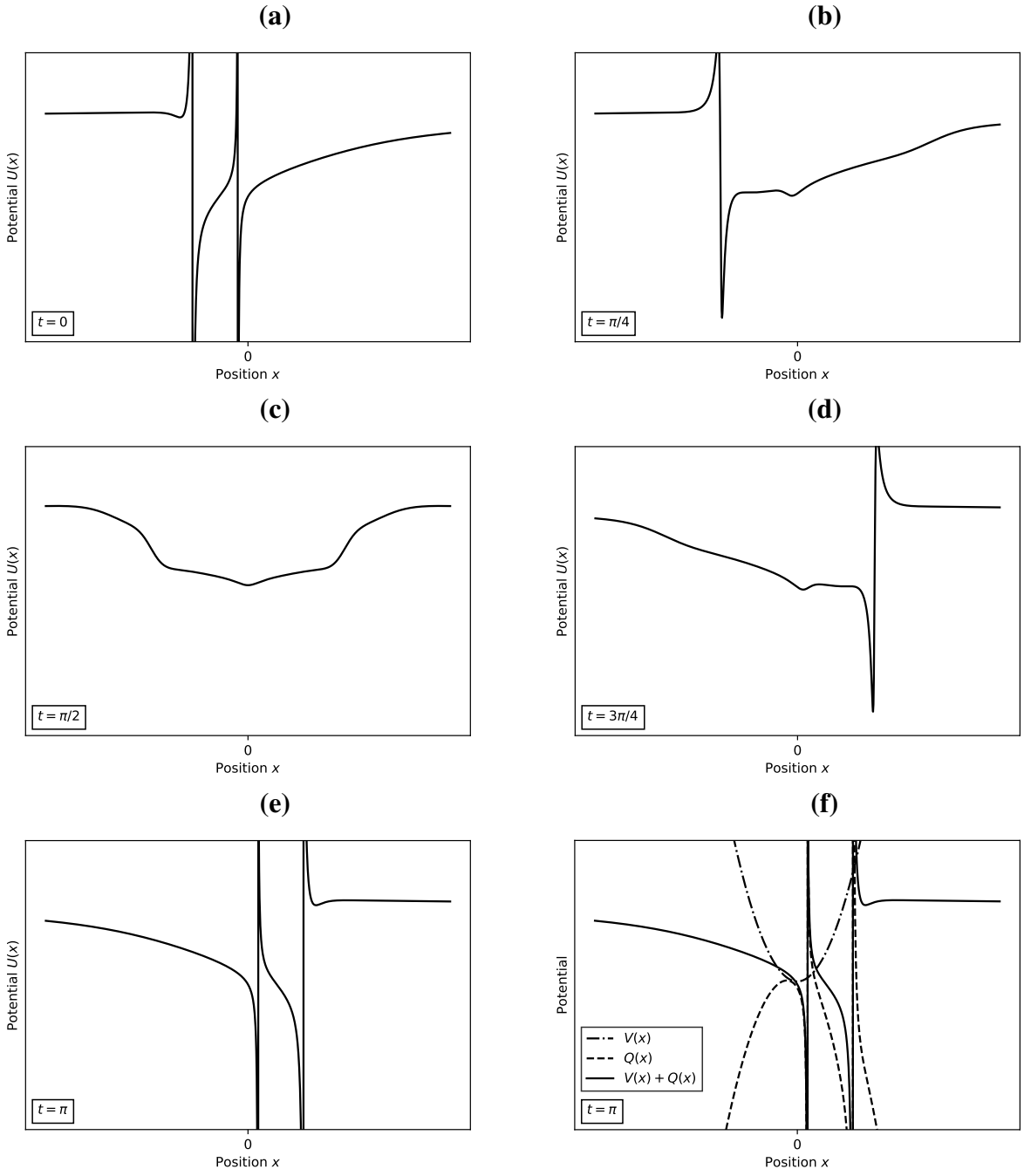

Figure 2.10 In frames 2.10a through 2.10e the total potential $U(x,t)$ corresponding to the coherent state $\Psi^1(x,t)$ is plotted in time increments of $\pi/4$ for $0 \leq t \leq \pi$. In frame 2.10f, the total potential is plotted alongside the quantum and classical potentials at time $t = \pi$ for completeness, showing that $U(x,t) = V(x,t) + Q(x,t)$.

of states previously considered. Again we see a region of considerable movement surrounded by regions of near immobility, centered around the origin. Despite arising from a combination of coherent states, the trajectories are decidedly non-oscillatory in the sinusoidal sense we tend to consider classically, being even less oscillatory than those shown in Figure 2.3. Instead we see simultaneous movement in opposing directions, with no trajectories ever crossing the origin. The general form of a given trajectory is determined by whether it falls to the left or to the right of the origin. The interested reader can reference [3] to see additional examples of trajectories for states in which distinct measurement outcomes are determined by the initial position of a particle relative to some critical dividing trajectory, showing that this feature is common in Bohmian analysis of quantum states.

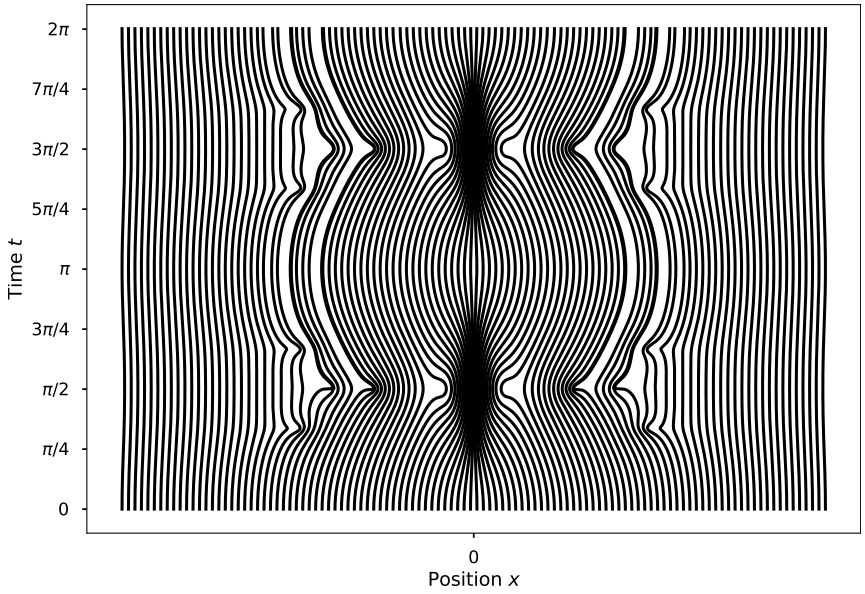

Figure 2.11 Bohmian trajectories for an approximation of the even cat state $\Psi^1_{even}(x,t)$. Note the numerical instabilities.

The total potential corresponding to the even cat state is shown in Figure 2.12. In this case we see a closer correspondence between the potential and the trajectories. However, we will still limit ourself to a brief discussion regarding the general features of the potential.

First, note that the potential has a period of length π, as do the trajectories. In our analysis of previous potentials, we have seen that the potential to the right of the origin behaves in the same

way as the potential to the left of the origin, with a phase difference of π. Thus, the potentials (and so also the corresponding trajectories) are symmetric in space with a phase shift across the origin. In the present case, the right- and left-hand sides of the potential are symmetric in space without a phase shift, and this symmetry is preserved as the frames advance, so that for the right-hand side to take on the aspect of the left-hand side after a space of time of $\Delta t = \pi$ is simply to repeat itself, giving rise to the observed doubling of periodicity.

As for the actual form of the potential, we see that at time $t = 0$ the potential has negative derivative to the left and positive derivative to the right, implying that all trajectories will display acceleration towards the origin. This potential remains relatively constant through frame 2.12b until frame 2.12c, where the derivative's sign is inverted abruptly throughout the potential. In frames 2.12d through 2.12e we see these steps invert themselves so that by time $t = \pi$ the situation is identical to that in frame 2.12a. This behavior in the potential implies a periodic symmetric contraction and expansion of trajectories, exactly as is seen in Figure 2.11.

It is also interesting to note that in frame 2.12c the presence of singularities facilitates the movement of a particle from a region of lower potential to a region of higher potential without the particle needing to have momentum sufficient to carry it into the higher potential region. This effect is something not seen in classical mechanics, and analysis of its importance and meaning in a Bohmian context could be an interesting future research question.

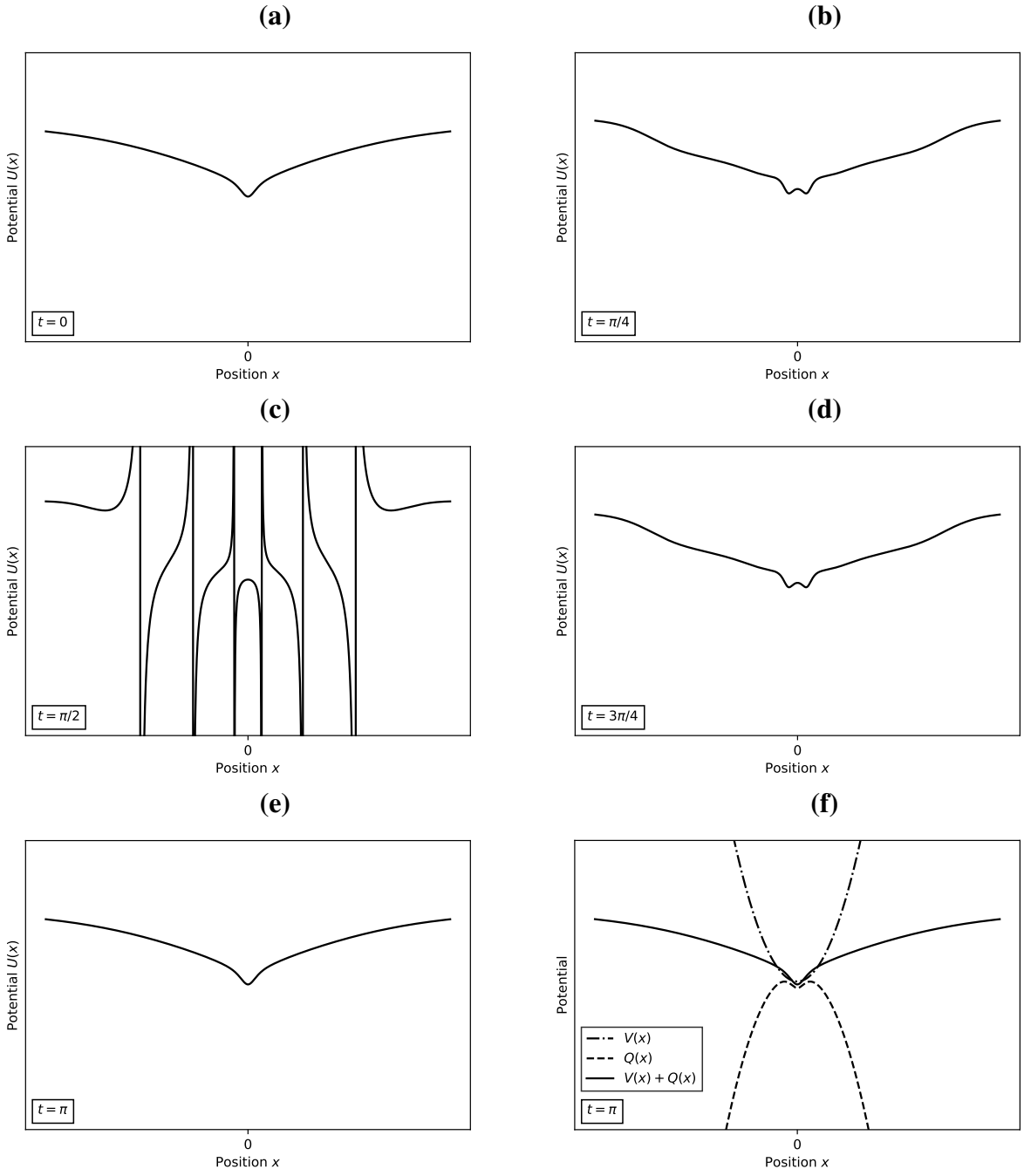

Figure 2.12 In frames 2.12a through 2.12e the total potential $U(x,t)$ corresponding to the cat state $\Psi^1_{even}(x,t)$ is plotted in time increments of $\pi/4$ for $0 \leq t \leq \pi$. In frame 2.12f, the total potential is plotted alongside the quantum and classical potentials at time $t = \pi$ for completeness, showing that $U(x,t) = V(x,t) + Q(x,t)$.

Chapter 3

Conclusion

We have now shown in some detail how Bohmian mechanics provides us with an intuitively accessible set of tools through which to view the quantum theory, namely the dynamical relationship between the quantum potential and the trajectories. It is easy to see how this approach to quantum mechanics would be more readily understood by students of physics having taken a course in Newtonian mechanics. As discussed in Section 2.1, Bohmian mechanics in practice solves the Schrödinger equation as is done in standard quantum mechanics and the trajectory information is extracted from the wave function. Thus, a student trained in Bohmian mechanics will be well versed in using the tools and techniques of standard quantum mechanics.

We have also seen that the Bohmian view in no way eliminates the nonclassical aspects of quantum theory. In fact, nonlocality plays a central role [3]. The difference between Bohm's formulation and the standard formulation is that Bohm provides an intuitive and self-consistent picture of microscopic phenomena, with all nonclassical effects essentially due to the quantum potential (2.6). To take (2.7) seriously is simply to favor an interpretation which is intuitive, which goes beyond an epistemology of microscopic phenomena, and which opens a door to future discovery.

Appendix A

Assumptions of Bell's Inequality

Details regarding Bell's derivation of his inequality can be found in his original work [23]. The purpose of this section is to outline briefly his derivation and show in detail how his work depends simultaneously on the assumptions of locality and realism. The CHSH inequality is derived from Bell's original inequality [24], and so also depends critically on these assumptions. Thus, so does the interpretation of the results of any experiment based on either inequality.

Formulation

Let Γ be the vector space of all possible combinations of local hidden variables, and let $\lambda \in \Gamma$. Assume λ is distributed according to $\rho(\lambda)$. Bell's derivation uses the quantities

$$A(\mathbf{a},\lambda) = \pm 1, \quad B(\mathbf{b},\lambda) = \pm 1 \tag{A.1}$$

to represent the results of spin measurements made in directions **a** and **b** by two parties on a pair of entangled particles. The correlation function is defined as

$$P(\mathbf{a},\mathbf{b}) = \int_{\Gamma} \rho(\lambda) A(\mathbf{a},\lambda) B(\mathbf{b},\lambda) d\lambda, \tag{A.2}$$

where

$$\int_\Gamma \rho(\lambda) = 1. \tag{A.3}$$

For the singlet state, where the intrinsic spin is opposite for both particles,

$$P(\mathbf{a},\mathbf{a}) = -1 \implies B(\mathbf{a},\lambda) = -A(\mathbf{a},\lambda) \tag{A.4}$$

$$\implies P(\mathbf{a},\mathbf{b}) = -\int_\Gamma \rho(\lambda) A(\mathbf{a},\lambda) A(\mathbf{b},\lambda) d\lambda. \tag{A.5}$$

From this, some algebraic manipulation on the expression

$$P(\mathbf{a},\mathbf{b}) - P(\mathbf{a},\mathbf{c})$$

yields

$$|P(\mathbf{a},\mathbf{b}) - P(\mathbf{a},\mathbf{c})| + P(\mathbf{b},\mathbf{c}) \leq 1, \tag{A.6}$$

the final result.

Locality

Bell assumes locality by assuming that A is a function of $\mathbf{a}$ only, and not of $\mathbf{b}$, and that B is a function of $\mathbf{b}$ only, and not of $\mathbf{a}$. To see how (A.6) depends on this assumption, we will attempt to carry out the derivation without assuming locality.

Replace (A.1) by

$$A(\mathbf{a},\mathbf{b},\lambda) = \pm 1, \quad B(\mathbf{a},\mathbf{b},\lambda) = \pm 1.$$

Equation (A.2) becomes

$$P(\mathbf{a},\mathbf{b}) = \int_\Gamma \rho(\lambda) A(\mathbf{a},\mathbf{b},\lambda) B(\mathbf{a},\mathbf{b},\lambda) d\lambda.$$

However, under this reformulation,

$$P(\mathbf{a},\mathbf{a}) = -1 \implies B(\mathbf{a},\mathbf{a},\lambda) = -A(\mathbf{a},\mathbf{a},\lambda) \neq -A(\mathbf{a},\mathbf{b},\lambda).$$

Without equality, we cannot conclude

$$P(\mathbf{a},\mathbf{b}) = -\int_{\Gamma} \rho(\lambda) A(\mathbf{a},\mathbf{b},\lambda) B(\mathbf{a},\mathbf{b},\lambda) d\lambda,$$

an essential step in the derivation. Compare this step to (A.4, A.5) above.

Realism

Bell assumes realism by assuming that the integral in (A.3) exists. Treatment of this assumption is much simpler than that of locality. To assume non-realism, we simply forfeit (A.3). Without this assumption, we cannot even begin to construct (A.2), so the derivation is stopped before it is begun.

Appendix B

Proof of Non-crossing of Bohmian Trajectories

Bohmian mechanical trajectories cannot cross. For this reason, Bohmian mechanics is often referred to as the *hydrodynamic interpretation* of quantum mechanics, since the arrangement of the trajectories is similar to the flow lines of hydrodynamic current. This correspondence is explored more deeply by Robert Wyatt [15].

Additional discussion regarding the non-crossing of Bohmian trajectories and the precise relation between this principle and quantum theory is provided by Peter Holland [11]. Here, we will limit ourselves to the outlining of a simple argument supporting the fact that trajectories cannot cross. This is not a rigorous proof, but rather an argument meant to show the reader one possible way of understanding the problem.

Let $\mathbf{x}_n : \mathbb{R} \longrightarrow \mathbb{R}^3$ be the position of the nth particle as a function of time t (i.e. $\mathbf{x}_n$ is the trajectory of the nth particle) and let $\mathbf{v} : \mathbb{R}^4 \longrightarrow \mathbb{R}^3$ be the velocity field for the system. We can write the velocity corresponding to the nth trajectory as $\mathbf{v}_n(t) = \mathbf{v}(\mathbf{x}_n(t), t)$.

Since velocity is the time derivative of position, we can write

$$\mathbf{v}_n = \frac{d\mathbf{x}_n}{dt} = \lim_{\delta t \to 0} \frac{\mathbf{x}_n(t+\delta t) - \mathbf{x}_n(t)}{\delta t}.$$

From this, we can deduce the approximate relationship

$$\mathbf{x}_n(t+\delta t) \approx \mathbf{x}_n(t) + \delta t\, \mathbf{v}_n(t), \tag{B.1}$$

which becomes becomes an equality in the limit as $\delta t \to 0$.

Now, if we assume that there exists a time t_0 such that $\mathbf{x}_1(t_0) = \mathbf{x}_2(t_0)$ (i.e. that $\mathbf{x}_1$ and $\mathbf{x}_2$ cross), then by application of (B.1) we obtain

$$\lim_{\delta t \to 0} \mathbf{x}_1(t_0+\delta t) = \lim_{\delta t \to 0} \mathbf{x}_1(t_0) + \delta t\, \mathbf{v}_1(t_0) = \lim_{\delta t \to 0} \mathbf{x}_1(t_0) + \delta t\, \mathbf{v}(\mathbf{x}_1(t_0), t_0)$$

$$= \lim_{\delta t \to 0} \mathbf{x}_2(t_0) + \delta t\, \mathbf{v}(\mathbf{x}_2(t_0), t_0) = \lim_{\delta t \to 0} \mathbf{x}_2(t_0) + \delta t\, \mathbf{v}_2(t_0) = \lim_{\delta t \to 0} \mathbf{x}_2(t_0+\delta t).$$

This shows that $\mathbf{x}_1$ and $\mathbf{x}_2$ must be equal over an infinitesimal time step. However, this is true for any $t_l = t_m + \delta t$, and the value of the trajectory $\mathbf{x}_n$ at a given time is the integration over an infinite number of such infinitesimal time steps. Thus, $\mathbf{x}_1$ and $\mathbf{x}_2$ must be equal for all t.

Bibliography

[1] Albert Einstein, Boris Podolsky, and Nathan Rosen. “Can Quantum-Mechanical Description of Physical Reality Be Considered Complete?” *Physical Review* 47 (1935), p. 777. DOI: 10.1103/PhysRev.47.777.

[2] E. T. Jaynes. “Clearing Up Mysteries - The Original Goal”. *Maximum Entropy and Bayesian Methods. Cambridge, England, 1988*. International MAXENT Workshop. Kluwer Academic Publishers, 1989, pp. 1–27.

[3] David Bohm and Basil J. Hiley. *The Undivided Universe. An Ontological Interpretation of Quantum Theory*. Routledge, 1993. ISBN: 9780415065887.

[4] David Bohm. “A Suggested Interpretation of the Quantum Theory in Terms of “Hidden” Variables. I and II”. *Physical Review* 85.2 (1952), pp. 166, 180. DOI: 10.1103/PhysRev.85.166;10.1103/PhysRev.85.180.

[5] J. R. Barker, R. Akis, and D. K. Ferry. “On the Use of Bohmian Trajectories for Interpreting Quantum Flows in Quantum Dot Structures”. *Superlattices and Microstructures* 27.5/6 (2000), p. 319. DOI: 10.1006/spmi.2000.0834.

[6] A. S. Sanz, F. Borondo, and S. Miret-Artés. “Causal Trajectories Description of Atom Diffraction by Surfaces”. *Physical Review B* 61.11 (2000), p. 7743. DOI: 10.1103/PhysRevB.61.7743.

[7] Z. S. Wang, G. R. Darling, and S. Holloway. "Dissociation Dynamics from a de Broglie-Bohm Perspective". *Journal of Chemical Physics* 115.22 (2001), p. 10373. DOI: 10.1063/1.1415450.

[8] Gary E. Bowman. "Quantum-mechanical time evolution and uniform forces". *Journal of Physics A* 39.1 (2005), p. 157. DOI: 10.1088/0305-4470/39/1/011.

[9] M. D. Towler, N. J. Russell, and Antony Valentini. "Time scales for dynamical relaxation to the Born rule". *Proceedings of the Royal Society* 468 (2012), p. 990. DOI: 10.1098/rspa.2011.0598.

[10] Siddhant Das and Detlef Dürr. "Arrival Time Distributions of Spin-1/2 Particles". *Scientific Reports* 9.2242 (2019). DOI: 10.1038/s41598-018-38261-4.

[11] Peter R. Holland. *The Quantum Theory of Motion. An Account of the de Broglie-Bohm Causal Interpretation of Quantum Mechanics*. Cambridge, 1993. ISBN: 9780521485432.

[12] Gary E. Bowman. "Bohmian mechanics as a heuristic device: Wave packets in the harmonic oscillator". *American Journal of Physics* 70.3 (2002), p. 313. DOI: 10.1119/1.1447539.

[13] Matthew Lawyer and Jean-François Van Huele. "Continuous Trajectories for the Quantum Harmonic Oscillator" (2020). To be published in the Journal of the Utah Academy of Science, Arts, and Letters.

[14] Roderich Tumulka. "Understanding Bohmian mechanics: A dialogue". *American Journal of Physics* 72.9 (2004), p. 1220. DOI: 10.1119/1.1748054.

[15] Robert E. Wyatt. *Quantum Dynamics with Trajectories. Introduction to Quantum Hydrodynamics*. Springer, 2005. ISBN: 9780387229645.

[16] David Bohm. *Quantum Theory*. Prentice Hall, 1951. ISBN: 9780137478736.

[17] Louis de Broglie. "La mecanique ondulatoire et la structure atomique de la matiere et du rayonnement". *Journal de Physique et le Radium* 8 (1927), p. 225. DOI: 10.1051/jphysrad:0192700805022500.

[18] Louis de Broglie. “La Nouvelle Dynamique des Quanta”. *Electrons et Photons. Rapports et Discussions du Cinquieme Conseil de Physique*. Institut International de Physique Solvay. Gauthier-Villars, 1928, pp. 105–141.

[19] Nathan Rosen. “On Waves and Particles”. *Journal of the Elisha Mitchell Scientific Society* 61.1 (1945), p. 67. ONLINE: https://www.jstor.org/stable/24333869.

[20] James Albertson. “Von Neumann’s Hidden-Parameter Proof”. *American Journal of Physics* 29.8 (1961), p. 478. DOI: 10.1119/1.1937816.

[21] John von Neumann. *Mathematische Grundlagen der Quantenmechanik*. Springer-Verlag, 1932. English translation: Robert T. Beyer. *Mathematical Foundations of Quantum Mechanics* Princeton University Press, 1995, pp. 305-324. ISBN: 0691080038.

[22] John S. Bell. “On the Problem of Hidden Variables in Quantum Mechanics”. *Reviews of Modern Physics* 38.3 (1966), p. 447. DOI: 10.1103/RevModPhys.38.447.

[23] John S. Bell. “On the Einstein Podolsky Rosen Paradox”. *Physics* 1.3 (1964), p. 195. DOI: 10.1103/PhysicsPhysiqueFizika.1.195.

[24] John F. Clauser et al. “Proposed Experiment to Test Local Hidden-variable Theories”. *Physical Review Letters* 23.15 (1969), p. 880. DOI: 10.1103/PhysRevLett.23.880.

[25] Christopher C. Gerry and Peter L. Knight. “Introductory Quantum Optics”. Cambridge University Press, 2008. Chap. Optical test of local realistic theories and Bell’s theorem. ISBN: 9780521527354.

[26] Alain Aspect, Philippe Grangier, and Gerard Roger. “Experimental Tests of Realistic Local Theories via Bell’s Theorem”. *Physical Review Letters* 47.7 (1981), p. 460. DOI: 10.1103/PhysRevLett.47.460.

[27] Alain Aspect, Jean Dalibard, and Gerard Roger. "Experimental Test of Bell's Inequalities Using Time-Varying Analyzers". *Physical Review Letters* 49.25 (1982), p. 1804. DOI: 10.1103/PhysRevLett.49.1804.

[28] Gregor Weihs et al. "Violation of Bell's inequality under strict Einstein locality conditions". *Physical Review Letters* 81.23 (1998), p. 5039. DOI: 10.1103/PhysRevLett.81.5039.

[29] C. Abellan et al. "Challenging local realism with human choices". *Nature* 557.7704 (2018), p. 212. DOI: 10.1038/s41586-018-0085-3.

[30] H. Goldstein, C. P. Poole, and J. L. Safko. *Classical Mechanics*. Addison-Wesley, 2001. ISBN: 9780201657029.

[31] David J. Griffiths. *Introduction to Quantum Mechanics*. Prentice Hall, 2005. ISBN: 9780131118928.

Index